

Order-Disorder Events Produced by Single-Vacancy Migration. II*

J. R. BEELER, JR.

Nuclear Materials and Propulsion Operation, General Electric Company, Cincinnati, Ohio

(Received 12 November 1964; revised manuscript received 18 January 1965)

Order-disorder processes caused by single-vacancy migration in orderable AB systems with cubic structure were studied in a series of computer experiments based on the Flinn-McManus Monte Carlo method. Single-vacancy migration was simulated within a crystal volume containing up to 2.2×10^6 atoms, this upper limit being imposed by the computer memory capacity. No constraints were placed upon either the shape or the connectivity of the migration region. In simple cubic (sc) and bcc systems, the presence of an ordering energy contracted the vacancy-migration region relative to that for a symmetric random walk (zero-ordering energy). This contraction was negligible in the fcc system. During ordering in the sc and bcc systems, the migration region tended to evolve as a mosaic of contiguous antiphase domains. In contrast, this region evolved as a collection of disjoint ordered centers in the fcc system. In addition, the ordering rate (per vacancy jump) in the sc and bcc systems was faster than that in the fcc system. Local fluctuations in the initial state of order exerted a profound influence upon the course of the ordering process. The Flinn-McManus model appears to give results which are qualitatively consistent with a variety of experimental observations.

1. INTRODUCTION

THIS article describes Monte Carlo computer experiments on single-vacancy migration in orderable AB alloys with cubic structures. Results of a similar study for the square planar (sp) lattice were reported earlier.¹ The term " AB alloy" denotes a system containing equal numbers of A and B atoms. Orderable alloys are those which exhibit states of long-range order (LRO) wherein each constituent atom type tends to be located on a specific subset of lattice sites rather than randomly distributed over the totality of lattice sites. Our intent, in this work, was to explore the implications of the Flinn-McManus Monte Carlo method² regarding the way single migration and the ordering (disordering) process influence one another in a regular³ lattice system. The focus of interest was centered on the character of the *initial* changes occurring in an orderable system, originally in an equilibrium state, after it had been subjected to a sudden temperature change. The specific characteristics treated are: (1) the crystal volume, (2) the configurational energy change, and (3) the ordered-nucleus formation modes, associated with a single vacancy migration history of N jumps.

Assuming the vacancy mechanism for atomic rearrangements, Flinn and McManus² studied both the approach to an equilibrium LRO state and the equilibrium LRO state *per se* in a regular AB bcc system. This system exhibits the B_2 superlattice^{4,5} in the fully

ordered state. Their computations were performed using a fixed-volume computational cell containing 2000 lattice sites and, in effect, periodic boundary conditions. The use of a cell with periodic boundary conditions, however, precludes a study of the growth of individual ordered nuclei. In the present study, the volume of the crystal affected by vacancy movement was allowed to expand freely in space with no constraints on either its shape or connectivity, as would be the case in a real alloy exhibiting an isotropic antiphase domain⁵ (APD) structure. This approach permits one to simulate the formation or decomposition of ordered centers and/or APD's as a consequence of atomic rearrangement via single-vacancy migration. Divacancy migration should also contribute to order-disorder processes but the much more complicated behavior of this defect is beyond the scope of this discussion. The computations were restricted to vacancy migration via a sequence of first-neighbor jumps, the mode indicated by Johnson's calculations for bcc and fcc metals.⁶ However, it has been suggested that second-neighbor jump processes could be important in alloys with a bcc structure at temperatures below the critical temperature.²

The qualitative nature of order-disorder processes in the sp system (Ref. 1) was also found in the simple cubic (sc) and bcc systems, but not in the fcc system. The superlattices of sp, sc, and bcc AB systems can be decomposed into two equivalent sublattices such that all A atoms reside on one of these sublattices and all B atoms on the other. In this state, the occupancy of sites on any straight or zig-zag line connecting nearest-neighbor positions, i.e., such as the vacancy-migration path line, forms a perfectly alternating series $A-B-A-B$ -, etc. We will refer to such a system as an alternating (ALT) system.⁷ It is not possible to describe the superlattice for the fcc AB system in terms of two equivalent

* This work was supported by the U. S. Atomic Energy Commission Contract No. AT(40-1)-2847 and the U. S. Air Force, Aeronautical Systems Division, Air Force Systems Command, Contract No. AF 33(657)-8473.

¹ J. R. Beeler, Jr. and J. A. Delaney, *Phys. Rev.* **130**, 962 (1963).

² P. A. Flinn and G. M. McManus, *Phys. Rev.* **124**, 54 (1961).

³ C. Domb, *Advan. Phys.* **9**, 149, 245 (1960). A regular system (assembly) is defined on p. 154. Briefly it is a system which can be characterized by specifying the occupancy, number, and geometry of occupiable sites, and its energy is the sum of first-neighbor interactions.

⁴ L. Guttman, *Solid State Phys.* **3**, 146 (1956).

⁵ M. J. Marcinkowski, in *Electron Microscopy and Strength of Crystals*, edited by G. Thomas and J. Washburn (Interscience Publishers, Inc., New York, 1963), pp. 333-440.

⁶ R. A. Johnson and E. Brown, *Phys. Rev.* **127**, 446 (1962); **134**, A1329 (1964).

⁷ See Ref. 3, p. 158.

sublattices. In the perfectly ordered state of this system every other (002) plane is occupied exclusively by one type of atom, as is also the case for the *B2* superlattice of the bcc system. However, the $\langle 111 \rangle$ nearest-neighbor jump directions in the bcc system do not lie in (002) planes, whereas some of the $\langle 110 \rangle$ nearest-neighbor jump directions in the fcc system do lie in (002) planes. Hence, there exists straight and zig-zag lines connecting nearest-neighbor sites in the fcc *AB* system superlattice on which the atom type does not alternate. A system with this character will be called a nonalternating (NALT) system.

The essential physical distinction between the two systems is that a vacancy can execute an *unlimited* series of nearest-neighbor jumps on one of the all-*A*-atom or all-*B*-atom planes in an ordered NALT system without changing the configurational energy, but this behavior is impossible in an ordered ALT system. For this reason we extend the definition of an ALT system to include the "imperfect" *B2* superlattice⁵ for an *A₃B* alloy wherein one sublattice is occupied solely by *A* atoms and the other is randomly occupied by *A* and *B* atoms. In this superlattice, a long series of vacancy jumps, each involving no configurational energy change is very improbable rather than strictly impossible. In this regard, Marcinkowski⁵ has pointed out that the features of the perfect and imperfect *B2* superlattice should be quite similar.

2. COMPUTATIONAL MODEL AND PROCEDURE

Flinn and McManus² specifically designed a Monte Carlo technique to approximate the kinetics of single-vacancy movement in orderable systems. In their model, a particular vacancy-jump direction is determined by a two-part rejection technique: (1) an atom on one of the *z* first-neighbor sites of the vacancy is selected at random; (2) the probability *p* for a vacancy jump into this site is then taken to be

$$p = e^{\Delta n \phi} / (1 + e^{\Delta n \phi}), \quad (1)$$

where Δn is the gain in the number of *AB* bonds associated with this event and $\phi = v/kT$. *k* is Boltzmann's constant, *v* the magnitude of the ordering energy and *T* the absolute temperature. This two-part cycle is repeated until a jump occurs. Whenever a jump occurred, in our calculations, the computer recorded any occupancy change, any configurational energy change, the new vacancy position and the number of rejection-technique cycles required to accomplish the jump. Occupancy maps for each (002) plane were also printed and the current long-range order (LRO) and short-range order (SRO) of the migration region were computed.

The Flinn-McManus model is the only practicable Monte Carlo method available for describing vacancy migration in orderable systems, which satisfies the *necessary* conditions for eventual attainment of the

equilibrium state. However, no formalism exists for estimating how closely the results of a model satisfying these conditions approximate reality. This circumstance is discussed in Sec. 8. We have extended the exploration of results from the Flinn-McManus model beyond those for a fixed-volume computational cell, by applying it to a freely expanding migration region, first in two dimensions (Ref. 1) and now in three dimensions. This has given a variety of results that can be compared with experiment.

The configurational energy of a regular system is taken to be the sum of first-neighbor interaction energies. Recent theoretical and experimental work indicates that the regular lattice-system approximation is a good one in the case of β brass. Equilibrium-state computer calculations by Guttman⁸ and by Flinn and McManus,² based on this model, give a temperature for the specific-heat maximum for β brass which is in good agreement with experiment. Walker and Keating⁹ find that their neutron diffuse-scattering data for β brass are consistent with a nearest-neighbor interaction model. Harrison and Paskin¹⁰ computed the ordering energy of β brass using Mott's "polar model" of an alloy and recently developed techniques for treating electron screening.¹¹ They found the ordering energy to be long range and oscillatory, rather than short range. However, Paskin¹² subsequently showed that the average order generated by the nearest-neighbor and long-range oscillatory interaction is approximately the same. He concluded that average characteristics are well approximated by nearest-neighbor statistical treatments.

Physically, the Monte Carlo experiments described here correspond to watching vacancy movement subsequent to a sudden temperature change. Recent experimental work of a parallel nature has been reported by Weisberg and Quimby¹³ and by Nagy *et al.*¹⁴⁻¹⁶ Earlier work includes the classical experiments of Burns and Quimby¹⁷ and of Sykes *et al.*¹⁸ The specimen was assumed to be in an equilibrium state characterized by the LRO parameter *S_i* for an initial temperature *T_i*. The temperature was then suddenly changed to *T* ≠ *T_i* and the migratory behavior of a single vacancy was followed as it participated in the establishment of the

⁸ L. Guttman, J. Chem. Phys. **34**, 1024 (1961).

⁹ C. B. Walker and D. T. Keating, Phys. Rev. **130**, 1726 (1963); D. T. Keating, Bull. Am. Phys. Soc. **9**, 242 (1964).

¹⁰ R. J. Harrison and A. Paskin, J. Phys. Radium **23**, 613 (1962).

¹¹ B. D. Silverman and P. R. Weiss, Phys. Rev. **114**, 989 (1959);

W. Kohn and S. H. Vosko, *ibid.* **119**, 912 (1960); R. J. Harrison and A. Paskin, J. Phys. Soc. Japan **15**, 1902 (1960).

¹² A. Paskin, Phys. Rev. **134**, A246 (1964).

¹³ L. R. Weisberg and S. L. Quimby, J. Phys. Chem. Solids **24**, 1251 (1963).

¹⁴ E. Nagy and I. Nagy, J. Phys. Chem. Solids **23**, 1605 (1962).

¹⁵ E. Nagy and H. Elkholy, J. Phys. Chem. Solids **23**, 1613 (1962).

¹⁶ E. Nagy and J. Tóth, J. Phys. Chem. Solids **24**, 1043 (1963).

¹⁷ F. Burns and S. L. Quimby, Phys. Rev. **97**, 1567 (1955).

¹⁸ C. Sykes and F. W. Jones, Proc. Roy. Soc. (London) **A157**, 213 (1936); **A166**, 376 (1938).

equilibrium state for T . At any "time," the site occupancy within the migration region was that determined by alterations in the initial occupancy state produced by the vacancy migration.¹⁹ The site occupancy in the environment of this region was that determined by S_i .

A detailed description of how the initial site occupancy was derived from S_i is given in Ref. 1; briefly the procedure is as follows: Subsets of lattice sites, L_a and L_b for A and B atoms, respectively, were defined for the perfectly ordered state. Given an initial state defined by S_i , the probability p_r that a site on either subset is rightly²⁰ occupied is

$$p_r = \frac{1}{2}(S_i + 1). \quad (2)$$

This procedure fully specifies the initial occupancy pattern only when $S_i = 1$. When $S < 1$, one must also specify the SRO. Flinn and McManus show that for $S > 0.8$, the first-neighbor SRO parameter σ is well-approximated by $\sigma = S^2$, a relation which follows from Eq. (2); hence, the initial state given by Eq. (2) is nearly correct for $S \geq 0.8$. Above the LRO critical temperature T_c , the quantity S vanishes, but σ is finite for all $T < \infty$. However, σ is very small for $T \gg T_c$ and sampling from $S_i = 0$ gives an approximately correct occupancy pattern. No method is known for occupancy sampling which *simultaneously* gives the correct equilibrium values of S and σ when $S < 1$. However, Gehlen and Cohen²¹ have recently worked out a Monte Carlo method for constructing an order state from and consistent with measured values of the LRO and the first three Warren-Cowley²² parameters.

For each assignment of S_i and ϕ , ten different pseudo-random-number sequences G_1, \dots, G_{10} were used to account in part for the SRO distribution associated with S_i . A single run was therefore specified by (S_i, ϕ, G_j) . The averaged results for 10 runs constituted the results of an experiment. Histories of $N = 10^4$ jumps could be run for $S_i = 0$, without exhausting the computer memory, and 3×10^4 jump histories were routinely possible for $S_i = 1$. The size of the crystal at which computer memory exhaustion occurred was $\sim 2.2 \times 10^5$ sites. This capacity was obtained by packing nine sites into each memory word.

3. MIGRATION EXTENT

One measure of single-vacancy migration extent is the average number of different lattice sites Σ visited by the vacancy in N jumps. This measure immediately gives the volume of material affected by vacancy migration and indicates the degree to which the vacancy

¹⁹ It is not possible to define an absolute time scale in the Flinn-McManus model. Hence, all "chronology" and "rate" statements are based on the number of vacancy jumps.

²⁰ A rightly occupied site is either an A atom on the L_a subset or a B atom on the L_b subset. A site otherwise occupied is wrongly occupied.

²¹ P. Gehlen and J. B. Cohen (to be published).

²² J. M. Cowley, Phys. Rev. **120**, 1648 (1960).

path retraces itself or, conversely, avoids retracing itself. Another measure of migration extent, directly connected with the vacancy diffusion coefficient D_v , is the mean-square displacement $\langle r^2 \rangle$ for N jumps. Because $D_v \propto \langle r^2 \rangle$, the effect of the ordering process on $\langle r^2 \rangle$ is associated with the correlation factor established by the ordering energy.

In AB alloys with cubic structure, Σ was found to be an approximately linear function of the number of vacancy jumps, provided the individual vacancy migration regions were isolated from one another. Our calculations gave the result,

$$\Sigma(N, S_i, \phi) = B(S_i, \phi, N) + C(S_i, \phi, N)N, \quad (3)$$

where S_i is the environmental LRO, associated with the initial temperature T_i , and T in $\phi = v/kT$ is the constant temperature of the alloy during the N -jump vacancy migration history. The N dependence of B and C was very weak for $N > 10^3$.

The fundamental references for judging the effect of an ordering energy upon Σ and $\langle r^2 \rangle$ are Σ_{rw} and $\langle r^2 \rangle_{rw}$ for a symmetric random walk ($\phi = 0$).^{23,24} Table I compares

TABLE I. $C = d\Sigma/dN$ for a symmetric random walk at $N = 10^4$ jumps as given by Monte Carlo experiments of 10 histories, of 10^3 histories and by Vineyard's asymptotic analysis.

Lattice	$N = 10^4$ 10 histories ^a	$N = 10^4$ 10^3 histories ^b	Vineyard ^c $N \rightarrow \infty$
sc	0.667	0.6641	0.6595
bcc	0.725	0.7216	0.7178
fcc	0.752	0.7472	0.7437

^a See Ref. 1.
^b See Ref. 23.
^c See Ref. 24.

the values of C_{rw} , given by 10-history¹ and 1000-history²³ computer experiments, for $N = 10^4$, with Vineyard's exact asymptotic values²⁴ for $N \rightarrow \infty$. Note that there is very little difference between Vineyard's asymptotic values of C_{rw} and those for $N = 10^4$. In the absence of an ordering energy, the probability for a vacancy to move to a previously unvisited site increases with the number of nearest neighbors. This underlying characteristic was retained, qualitatively, for $\phi > 0$, but the magnitude of Σ was markedly changed in the sc and bcc lattice. The variation of $d\Sigma/dN = C$ with S_i and ϕ for $N > 10^3$ is described in Figs. 1-3. Because $B \ll \Sigma$ and exhibits a weak N dependence, for large N , its behavior is not important and will not be discussed. The existence of a nonzero intercept for $\Sigma(N)$ is associated with the transition of the distribution for Σ from a non-normal to a normal distribution as N increases.²³

As mentioned in Sec. 1, the principal vacancy migration characteristics in the sc and bcc ALT lattices were quite similar and these characteristics were essentially

²³ J. R. Beeler, Jr., Phys. Rev. **134**, A1396 (1964).

²⁴ G. H. Vineyard, J. Math. Phys. **4**, 1191 (1963).

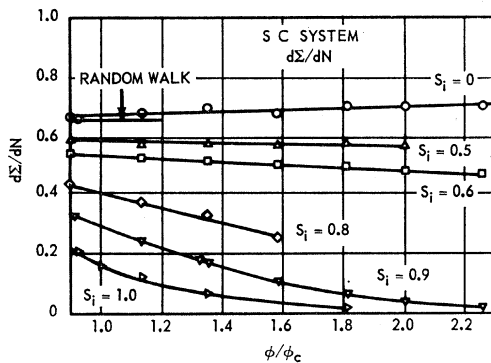


FIG. 1. $C = d\Sigma/dN$ for the sc system as a function of ϕ/ϕ_c (T_c/T) and S_i . Note that $C > C_{rw}$ for $S_i = 0$ and $\phi > 0$ in Figs. 1, 2, and 3.

different from those exhibited in the fcc NALT lattice. Because of this, the discussion will be largely centered about a description of vacancy migration in the bcc and fcc systems. For $S_i = 0$, $C(0, \phi)$ increased slightly with ϕ . This indicates that when a completely disordered alloy is quenched the ordering energy causes the migration region for N jumps to be slightly larger than that for a symmetric random walk of equal length, i.e., N jumps in a monatomic material with the same lattice geometry. In contrast, when $S_i = 1$, $C(1, \phi)$ decreased with increasing ϕ and $\Sigma < \Sigma_{rw}$. This contrast can be explained in terms of the configurational energy change per jump. When $S_i = 0$, the number of AB bonds gained per jump increases with increasing ϕ (see Sec. 4). This, together with the increase in Σ with ϕ , indicates that a vacancy tends to avoid re-entering a region previously visited when the LRO and SRO of the environment are small. It is, in this case, energetically more favorable for the vacancy to move into unexplored territory rather than re-enter old ground. When $S_i = 1$, however, a move into the unexplored perfectly ordered environment means a disruption of AB bonds and a consequent increase in crystal energy, except for jump directions in the planar L_a and L_b subsets in the ordered NALT fcc system. Consequently, the rate of migration region expansion is inhibited when $\phi > 0$, inhibition becoming progressively more severe as ϕ increases. A comparison of the magnitudes of $C = d\Sigma/dN$ in Fig. 3 for the fcc system with

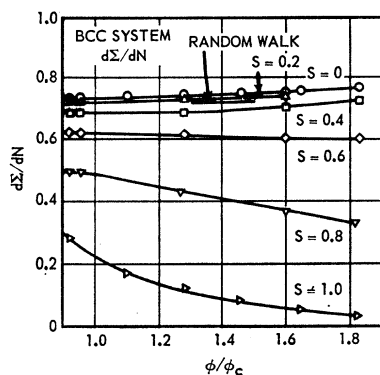


FIG. 2. $C = d\Sigma/dN$ for the bcc system.

those in Figs. 1 and 2 for the sc and bcc systems, respectively, shows this inhibition was much less severe in the fcc system.

A ratio called the contraction factor κ will be used to characterize the inhibition of vacancy migration caused by the presence of an ordering energy. κ is defined by Eq. (4) for Σ and $\langle r^2 \rangle$, the mean-square displacement:

$$\kappa(\Sigma) = \Sigma_{rw}/\Sigma, \quad (4a)$$

$$\kappa(r^2) = \langle r^2 \rangle_{rw}/\langle r^2 \rangle. \quad (4b)$$

The contraction factor indicates how much *larger* is the migration extent in a symmetric random walk than that in an orderable system. Figures 4 and 5 give $\kappa(\Sigma)$ and $\kappa(r^2)$, respectively, as functions of ϕ/ϕ_c for $S_i = 1$, where $\phi_c = v/kT_c$. The ratio $\kappa(r^2)/\kappa(\Sigma)$ appears in Fig. 6, for $S_i = 1.0$. Only a small contraction of Σ and $\langle r^2 \rangle$ occurred in the fcc system, but large contractions of ~ 30 for Σ and of ~ 60 for $\langle r^2 \rangle$ occurred in the sc and bcc systems. The dashed curve, "fcc ALT lattice" in Fig. 4 is for an *artificial* fcc system. It was obtained by instructing the computer to regard vacancy migration in a fcc system

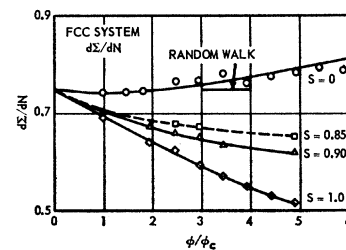


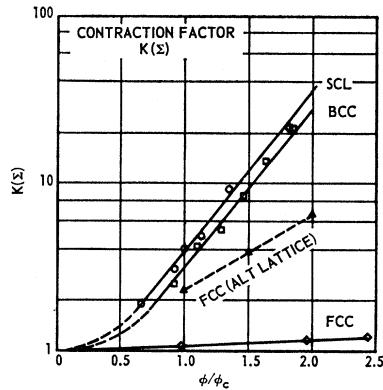
FIG. 3. $C = d\Sigma/dN$ for the fcc system. Note the expansion of the ordinate scale relative to that in the two previous figures. Note that the dashed curve ($S = 0.85$) is based on only three data points.

as being determined solely by the coordination number. The dashed and solid curves for the fcc system therefore serve to give an approximate separation between the effects of the changes in the coordination number and superlattice type associated with a change from the bcc to the fcc system. Each type of change appears to exert about the same influence in the over-all attenuation of $\kappa(\Sigma)$ for the fcc system, relative to that for the bcc system.

Figure 6 shows that $\kappa(r^2)$ was always greater than the $\kappa(\Sigma)$. This appears to arise from a truncation of the large- r tail of the $r(N)$ distribution in an ordered system, i.e., the ordered system $r(N)$ distribution is not given by a uniform compression toward the origin of that for a symmetric random walk. Kuper *et al.*²⁵ found that the measured atomic diffusion coefficients for Cu, Zn, and Sb in the ordered β brass were much smaller than the extrapolated diffusion coefficients for the high-temperature disordered state. The reduction factor at the lowest

²⁵ A. B. Kuper, D. Lazarus, J. R. Manning, and C. T. Tomizuka, Phys. Rev. **104**, 1536 (1956).

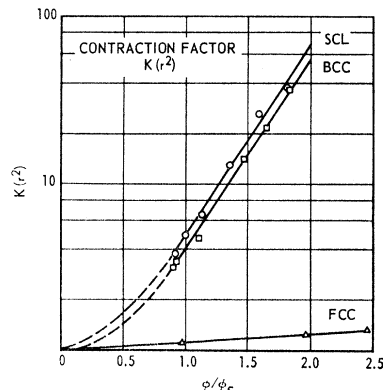
FIG. 4. Comparison of the contraction factors for Σ in the sc, bcc, and fcc systems when $S_i=1$. See text for an explanation of fcc (alternating lattice) curve.



measurement temperature ($T=0.73T_c$) was ~ 50 for Cu and ~ 250 for Zn. At this temperature, $\kappa(r^2)=15$. This seems to indicate that the purely order-induced contraction of $\langle r^2 \rangle$ for vacancy migration, although a contributing factor, is not the sole cause for the observed atomic diffusion coefficient attenuation in the ordered state. Note (Fig. 5) that $\kappa(r^2) > 1$ above the critical temperature and, therefore, is not purely a LRO effect. This behavior is consistent with the findings of Kuper *et al.* in that they observed the onset of a SRO effect at about 50°C above the critical temperature. The values quoted for $\kappa(r^2)$ are based on $\langle r^2 \rangle_{100}$ for successive 100-jump intervals in 10 000-jump histories. As the jump interval ΔN was increased, $\langle r^2 \rangle_{\Delta N}$ tended to fall off and hence the $\kappa(r^2)$ values given are lower bounds. The numerical ordering $\kappa(\text{fcc}) < \kappa(\text{bcc}) < \kappa(\text{sc})$ is in accord with the numerical ordering of C_{rv} for these lattices.

If, as suggested by Flinn and McManus, second-neighbor jumps occur in the ordered state of a bcc system, our values of $\kappa(\Sigma)$ and $\kappa(r^2)$ are too high. If second-neighbor jumps were, in fact, the dominant migration mode, the contraction factors for a bcc system would fall to the small values characteristic of the fcc system because second-neighbor jumps in an ordered bcc system are zero-energy change jumps. This would imply, as suggested by Flinn and McManus, that the increased activation energy required for second-

FIG. 5. Comparison of the contraction factors for $\langle r^2 \rangle$.



neighbor jumps is primarily responsible for the smaller diffusion coefficient in the ordered state, relative to the extrapolated value from the disordered state. Borg²⁶ considers that elastic constant changes, in the case of magnetic ordering, are the principal cause of atomic diffusion coefficient attenuation in the ordered state. Girifalco²⁷ has computed atomic diffusion coefficients for β brass on the basis of first-neighbor interactions and the vacancy diffusion mechanism. His results are in agreement with the data of Kuper *et al.* and, further, predict no change in the diffusion mechanism in going from the disordered to the ordered state.

4. CONFIGURATIONAL ENERGY

That part of the crystal energy which changes during either ordering or disordering is called the configurational energy E_c . The configurational energy increase which occurs when a perfectly ordered system ($S_i = \sigma_i = 1$) is made to disorder completely ($S = \sigma = 0$)

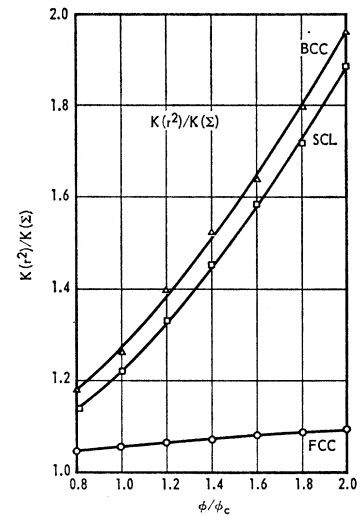


FIG. 6. Ratio $\kappa(r^2)/\kappa(\Sigma)$.

will be denoted by E_0 . Conversely, $-E_0$ is the configurational energy decrease associated with a change from complete disorder to perfect order. In this discussion, $\beta(S_i, \phi, N)$ denotes the number of AB bonds gained in N vacancy jumps, given S_i and ϕ . It turned out that β , like Σ , was a linear function of N , i.e., $\beta = b + cN$, and that the behavior of the intercept can be ignored, for large N , as can the N dependence of c . The configurational energy change ΔE_c associated with β is

$$\Delta E_c = -\beta v.$$

The quantity (β/Σ) indicates the extent to which the configurational energy change corresponds to the change associated with the transition from the initial equilibrium state characterized by S_i to that characterized

²⁶ R. J. Borg, J. Appl. Phys. 35, 567 (1964).

²⁷ L. A. Girifalco, J. Phys. Chem. Solids 24, 323 (1964).

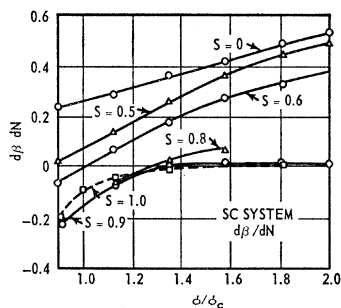


FIG. 7. $C=d\beta/dN$ for the sc system as a function of ϕ/ϕ_c and S_i . Contrast the irregular vertical positioning of the curves as a function of S_i in this and the succeeding figure, for the bcc system, to the regular positioning in Fig. 9 for the fcc system.

by ϕ , as shown by Eq. (6). E_0 is given by

$$E_0 = \frac{1}{2} z N' v \quad (\text{sc and bcc}), \quad (5a)$$

$$E_0 = \frac{1}{12} z N' v \quad (\text{fcc}), \quad (5b)$$

where N' is the number of lattice sites concerned.

Upon substituting the appropriate z values into Eq. (5) and identifying Σ with N' one obtains

$$\Delta E_c/E_0 = 2\beta/3\Sigma \quad (\text{sc}), \quad (6a)$$

$$\Delta E_c/E_0 = \beta/2\Sigma \quad (\text{bcc}), \quad (6b)$$

$$\Delta E_c/E_0 = \beta/\Sigma \quad (\text{fcc}). \quad (6c)$$

The SRO parameter σ is related to $\Delta E_c/E_0$ as

$$\Delta E_c/E_0 = (1 - \sigma). \quad (7)$$

For $S_i=1$ and $\phi=0$, E_c increased at the rate 1.75, 2.91, and 1.11 V per jump in the sc, bcc, and fcc lattices, respectively. This instance represents the disordering of a perfectly ordered crystal by a vacancy executing a symmetric random walk. Because $\phi=0$ corresponds to $T = \infty$, the case ($S_i=1, \phi=0$) cannot be physically realized if $v > 0$ for all temperatures. It could be approximated by heating to a temperature near the melting point.

Given $S_i=0$ and $\phi=2\phi_c$ ($T=T_c/2$), the quantity E_c decreased at a rate of -0.535 , -0.700 , and -0.390 V per jump, respectively, in the sc, bcc, and fcc lattices.

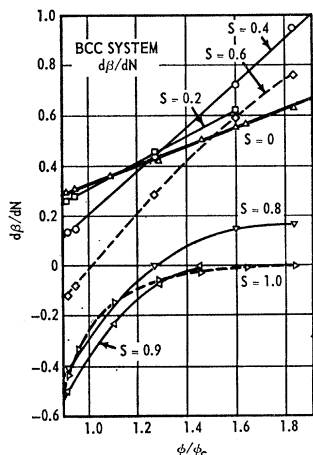


FIG. 8. $C=d\beta/dN$ for the bcc system.

This represents the ordering of a completely disordered alloy after being quenched to a temperature $T=T_c/2$. Figures 7-9 illustrate the behavior of $d\beta/dN$ as a function of ϕ/ϕ_c for various S_i . Again the general behaviors of the sc and bcc are similar and this behavior is different from that of the fcc system.

The degree to which a complete transition between equilibrium states was attained within the single-vacancy migration regions in the bcc system, during $\sim 10^4$ jumps was surprisingly large. In contrast, the progress toward equilibrium in the fcc system was meager. A plot of the ratio E_c/E_0 versus ϕ/ϕ_c , given by the periodic cell equilibrium state calculations of Flinn and McManus, appears in Fig. 10 along with that given by the present expanding migration region study. Curve A is the migration region configurational energy for disordering from $S_i=1$ in 3×10^4 jumps and curve B

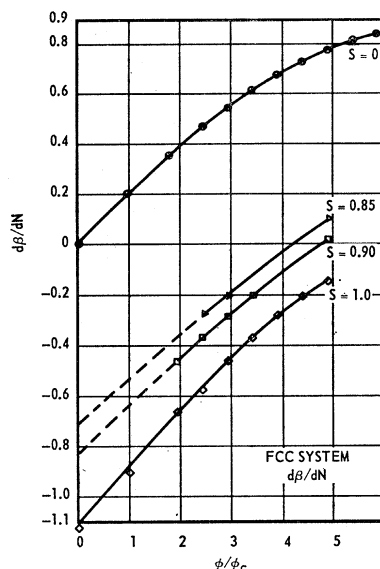


FIG. 9. $C=d\beta/dN$ for the fcc system.

that for ordering from $S_i=\sigma_i=0$ in 10^4 jumps. For $T < 0.8T_c$, disordering from $S_i=1$ to the equilibrium state for T was accomplished within a 3×10^4 jump migration region. Curve B for ordering from $S_i=\sigma_i=0$ runs smoothly into the equilibrium curve at $T=1.1T_c$ but lies above the equilibrium curve for $T < 1.1T_c$. The data for curve B were obtained from 10^4 jump histories. Over 87% of the configurational energy change for transition to an equilibrium state was attained in disordering to a temperature $T < T_c$. This indicates that either in disordering to the critical state from $S_i=1$ or ordering to the critical state from $S_i=0$ the major part of the transition is accomplished within isolated migration regions.

In this context disordering appeared to be largely a local, one-shot process. However, ordering from $S_i=\sigma_i=0$ at $T < T_c$ was not even approximately accomplished within an isolated migration region.

Figure 11 describes the fractional energy change accomplished by a single vacancy in the ordering process. It drops off rapidly below $1.1T_c$ and is roughly 0.4 below $0.83T_c$. This indicates that several traverses of the individual vacancy migration regions, after they have grown into contact, would be required to establish an ordered state. In particular, from Fig. 2 one sees that $d\Sigma/dN \simeq 0.75$ for $T < 1.1T_c$ and $S_i = 0$. This implies an average of 1.3 moves per atom in the migration region. Flinn and McManus² found that about 10 moves per atom are required for a complete disorder-order transition. Hence, it appears that 40% of the required configurational energy change is accomplished during the execution of the initial 13% of the required moves per atom. This clearly suggests that quenched-in excess vacancies should play a dominant role in the initial ordering process (during a quench) and that their progressive loss should very much slow down subsequent ordering stages. This is consistent with the experimental results of Clarebrough *et al.*,²⁸ Wechsler and Kernohan,²⁹ and Brooks and Stansbury.³⁰

Because of fluctuations in the vacancy concentration, the behavior of initially closely spaced excess vacancies should play an important role in the nucleation of ordered regions because one would expect early overlap among their migration regions. In this regard, Monte Carlo studies on defect annealing show a strong fluctuation effect.²³ In addition, some *two-dimensional* calculations were run for pairs, triplets and quartets of initially closely spaced single vacancies to estimate what effect these fluctuations might have on the initial ordering process. There was a tendency for a pair of vacancies to order the alloy at a faster rate in a total of N jumps than would a single vacancy in N jumps. Unfortunately, no vacancy-vacancy binding energy was instituted, hence the results after association were of no value with respect to estimating subsequent ordering effects by divacancies. Even without an explicit divacancy binding energy, two initially separated vacancies tended to stay within the vicinity of one another after overlap of their migration regions by virtue of the ordering energy. This behavior should carry over to the sc and bcc systems but not to the fcc system.

A comparison of the distributions for the AB bond gain Δn per jump for ALT and NALT systems clearly shows that the existence of zero-energy change paths in an ordered NALT lattice is responsible for the quasi-random walk migration behavior in this system. Approximate differential distributions were constructed from a clerical tally of the bond changes per jump for 500 randomly chosen jumps listed on the printout sheets for an experiment. The averages $\langle \Delta n \rangle = d\beta/dN$ given by these distributions were within $\pm 30\%$ of

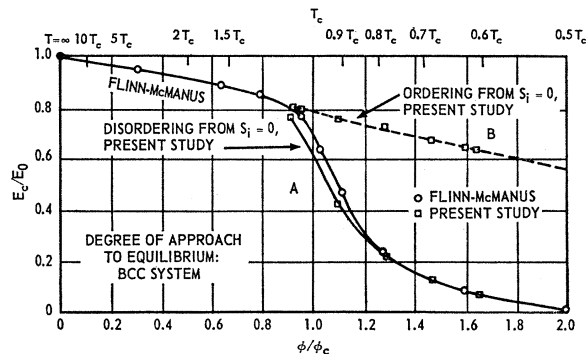


FIG. 10. Ratio of the configurational energy change E_c to E_0 as given by the present expanding-region calculations and as given by the Flinn-McManus fixed-volume equilibrium-state calculations, for the bcc system: (A) ordering from $S_i = 0$ in 10^4 jumps, present study, (B) disordering from $S_i = 1$ in 3×10^4 jumps, present study. Note the close approach to equilibrium in the expanding migration region for $\phi/\phi_c > 1.2$ (disordering) and $\phi/\phi_c < 0.95$ (ordering).

those given by the automatic cumulative tally made by the computer over the $N \geq 10^6$ jumps per experiment. Unfortunately, we were not sufficiently foresighted to include a Δn distribution routine in the computer program.

Differential Δn distributions for the bcc and fcc systems are plotted in Figs. 12–13 for disordering from $S_i = 1$ to $S = 0$. The bcc system distribution is for migration at $T = 1.1T_c$ and that for the fcc system is for $T = 1.02T_c$. Note that the distribution for the bcc system is *bimodal*, with only a small contribution from the vicinity of $\Delta n = 0$, while that for the fcc system is *unimodal* and the contribution from the vicinity of $\Delta n = 0$ is relatively large. This, in conjunction with $d\Sigma/dN(\text{fcc}) = 0.697 > d\Sigma/dN(\text{bcc}) = 0.284$, for the temperatures concerned, clearly indicates a strong self-avoidance tendency for the vacancy migration path in the fcc system and a tendency for migration path convolution and retracing in the bcc system. During disordering at temperatures $T \leq T_c$, the migration region

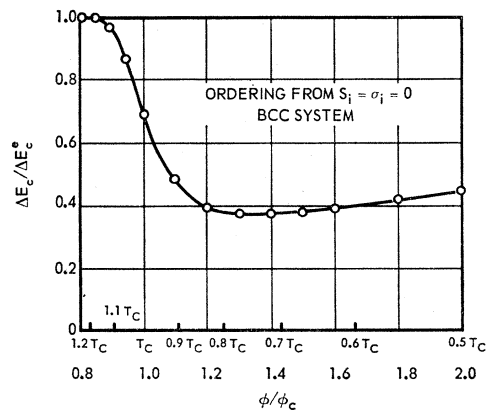


FIG. 11. Ratio of observed configurational energy change (ΔE_c) to that required to attain equilibrium (ΔE_c^e) during ordering from $S_i = 0$ in a bcc-system migration for 10^4 jumps.

²⁸ S. Matsuo and L. M. Clarebrough, *Acta Met.* **11**, 1195 (1963); L. M. Clarebrough, M. E. Hargreaves, and M. H. Loretto, *Proc. Roy. Soc. (London)* **A257**, 326, 338 (1960); **A261**, 500 (1961).

²⁹ M. S. Wechsler and R. H. Kernohan, *Acta Met.* **7**, 599 (1959).

³⁰ C. R. Brooks and E. E. Stansbury, *Acta Met.* **11**, 1303 (1963).

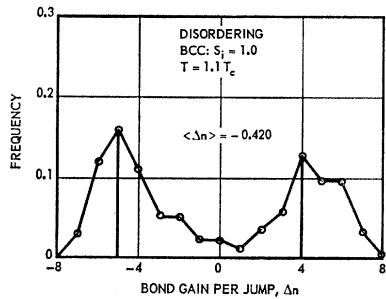


FIG. 12. Bimodal distribution for the AB -bond gain per jump (Δn) during disordering from $S_i=1$ in the bcc system. The distribution for the sc system was also bimodal.

in the bcc system was, from the onset, in nearly an equilibrium state (see Fig. 10) and approached the equilibrium state from the "ordered side," so to speak. In contrast, overly disordered (SRO) regions were initially created in the fcc system. If real, this circumstance would necessitate reordering in a subsequent stage of the disorder transition, and the equilibrium state would be approached from the "disordered side." Specifically, the ratio of $\langle d\beta/dN \rangle(\text{fcc}) = -0.446$ to the maximum bond loss per jump (-3) was 0.15 while that of $\langle d\beta/dN \rangle(\text{bcc}) = -0.432$ to the maximum bond loss per jump (-7) was 0.062. The Δn distributions for the sc system were also bimodal for disordering. During the ordering, the Δn distributions for the ALT lattices were again bimodal and that for the NALT lattice was unimodal.

A schematic representation of the vacancy path structure for ALT and NALT lattices, during ordering, is given by Fig. 14. In both instances the path structure was made up of localized curlicue patterns which were connected by semirandom walk tracks. The curlicues tended to be dense and closely spaced in the ALT lattices but open and widely separated, relative to their diameter, in the NALT lattice. In each instance, ordered centers were formed in the regions where each curlicue path occurred.

5. EFFECT OF FLUCTUATION CONFIGURATIONS

An attempt was made to correlate the variations in $d\Sigma/dN$ and $d\beta/dN$, as functions of S_i and ϕ , with fluctuations in the initial occupancy pattern. The completeness with which this could be done fell short of that which was possible in Ref. 1. No formal theory seems to exist for line form or volume shape analysis of digitalized data on $\sim 2 \times 10^5$ A and B atom positions in three dimensions.³¹ However, it was possible to show that fluctuation configurations in the initial occupancy pattern significantly influenced the course of the ordering process in the ALT systems. In this context, the term fluctuation configuration denotes a local region in which the relative numbers of rightly (R) and wrongly (W) occupied sites²⁰ deviate strongly from the

³¹ The vacancy-path forms and volume shapes with which we are concerned appear to be too convoluted and irregular, respectively, for an application of standard form-recognition techniques used to analyze high-energy particle-track data, for example.

relative numbers averaged over the entire crystal. In a recent discussion of the definition and determinability of order, Rudman³² emphasized the possible importance of local order fluctuations which escape detection in a conventional treatment of *averaged* pairwise correlations proceeding from a diffuse-scattering analysis, for example.

Two types of fluctuation configurations appeared to be important: (1) ordered nuclei, and (2) minority strings. An ordered nucleus is a small volume filled predominantly by either R sites or W sites and is therefore a localized low-energy region. A minority string is a short lineal configuration (not necessarily straight) of 5–10 sites which are *oppositely* occupied with respect to the majority of their first neighbors. Minority strings are, therefore, associated with localized, high-energy regions.

Figure 15 schematically illustrates minority strings in a $S_i=0$ matrix, and the combination of minority strings and ordered nuclei in a matrix with low but non-zero LRO. We have concluded that minority strings cause the slight enhancement of Σ and $\langle r^2 \rangle$ observed for $S_i=0$ and $\phi > 0$, relative to their values for a symmetric random walk. These strings function both as migration path short cuts and as nucleation centers for ordered nuclei and/or antiphase domains during vacancy migration. A minority string is effectively a one-way passage for vacancy travel which is automatically eradicated when traversed. This occurs because a forward jump along a string is strongly favored by the energy decrease associated with an AB -bond gain while a backward jump (retraction of the previous forward jump) tends to be prohibited by an energy increase of equal magnitude. Because of the strongly preferred forward motion, $d\Sigma/dN$ approaches unity along a minority string and Σ is enhanced. Enhancement of $\langle r^2 \rangle$ arises from both the one-way nature of the string passage and the random distribution of the minority string directions.³³ Owing to inhibited jump retraction, any vacancy following a minority string enjoys an increased *average* displacement per jump. In effect, a set of randomly directed unidirectional jump sequences of augmented average jump-length each aligned along

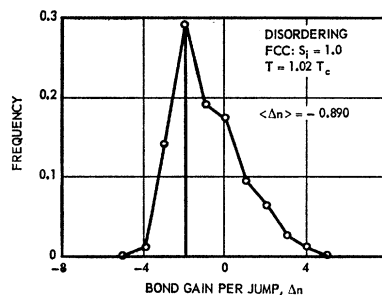


FIG. 13. Unimodal distribution for the AB -bond gain per jump during disordering from $S_i=1$ in the fcc system.

³² P. S. Rudman, *J. Met.* **16**, 78 (1964).

³³ The orientation of a minority string is that of a straight line connecting its ends.

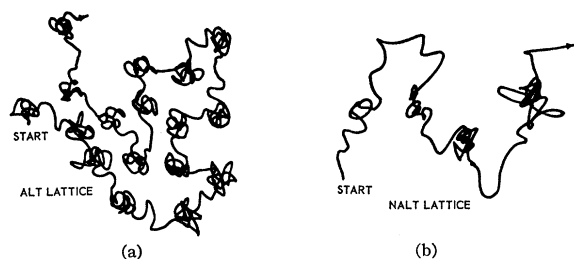


FIG. 14. Schematic representation of the vacancy-migration path structure during ordering from $S_i=0$ in (a) an alternating system, (b) a nonalternating system.

a minority string, becomes superposed on the ordinary jump migration process. This serves to increase the average jump-length squared and, perforce, $\langle r^2 \rangle$. This explanation is consistent with the observation that the enhancement of Σ and $\langle r^2 \rangle$ increased monotonically with ϕ in the experiments for $S_i=0$.

Low-energy ordered nuclei tended to inhibit vacancy migration by either reflection or trapping. When a vacancy encounters an ordered nucleus, penetration of this nucleus is not energetically favorable. In this sense the vacancy is reflected. Trapping can occur either at the surface of a highly ordered nucleus or inside a partially ordered nucleus. In each instance the basic behavior is the same, e.g., a high incidence of retracted jumps and circuitous path forms. Trapping on the boundary between two oppositely ordered nuclei³⁴ (antiphase domains) occurs because the migration process is there largely a zero-energy change random walk¹ which is confined to a closed surface. Surface trapping at the interface between a large, highly ordered nucleus and a partially ordered matrix proceeds from the tendency for the vacancy to add new ordered layers to this nucleus. Severe trapping can occur when a vacancy enters a large partially ordered nucleus through a relatively disordered zone. If, as it proceeds into the nucleus, the vacancy orders this zone, it becomes self-trapped in the interior of a highly ordered region. Once this occurs, migration becomes severely contracted, as in an ordered crystal, and escape from the nucleus is difficult.

Observe that $d\Sigma/dN$ for $S_i=0.2$ and 0.4 lie below but close to the curve for $S_i=0$. On the other hand, the curves for $S_i>0.4$ fall well below that for $S_i=0$. It appears that this occurs because both the size and density of ordered nuclei in the initial occupancy pattern increase with S_i . As was explained above, these regions tend to inhibit migration region expansion. For sufficiently large ϕ , the minority string effects are apparently strong enough to override the inhibition offered by small nuclei, either initially present or grown, and Σ rises above that for the random walk. The fact that the ϕ value at which this occurs for $S_i=0.2$ is smaller than the value of $S_i=0.4$ is consistent with this

³⁴ N. Brown and S. Cupchalk, Bull. Am. Phys. Soc. 8, 217 (1963).

TABLE II. Configurational energy change E_c^* and number of effective jumps N_{eff}^* associated with minority string eradication in the bcc system.

ϕ/ϕ_c	N_{eff}/N	$N_{\text{eff}}^*/N_{\text{eff}}$	E_c^*/E_c	E_c^*/N_{eff}^* (V)
(a) $S_i=0$				
0.9	0.80	0.08	0.56	-2.7
1.8	0.75	0.14	0.55	-2.7
(b) $S_i=1$				
0.9	0.45	0.17	...	-4.6
1.8	0.09	0.15	...	-5.3

explanation. For $S_i>0.4$, the inhibiting effect of larger ordered nuclei, either initially present or grown, completely dominates the migration expansion rate. In these instances the density of ordered nuclei is also sufficiently large that any minority strings in existence apparently serve merely to shuttle the vacancy from one nucleus to another.

In the course of N jumps in an ALT system, a vacancy makes a considerable number of retracted excursions during which no change occurs in either the occupancy pattern or configurational energy. Let $N_{\text{eff}} \leq N$ be the number of jumps in an N -jump history which are effective in producing either occupancy or configurational energy changes. The path traced out in these N_{eff} jumps will be called the effective path. A jump-by-jump study of the vacancy path for three 500-jump histories in the bcc system was made for ($S_i=0, \phi=\phi_c$), ($S_i=0, \phi=1.8\phi_c$), ($S_i=1, \phi=\phi_c$), and ($S_i=1, \phi=1.8\phi_c$). This analysis concerned the following quantities: N_{eff} , the number of effective jumps; N_{eff}^* , the number of effective jumps executed in following (eradicating) minority strings; and E_c^* , the configurational energy change associated with minority string eradication. Table II lists the results. In ordering from $S_i=0$, over half of the configurational energy change occurred during minority string eradication although less than 15% of the effective jumps were employed in string removal. The bond change per jump was 15 times larger along a minority string than that for ordinary effective jumps for $\phi=\phi_c$; a ratio of 7 to 1 occurred for $\phi=1.8\phi_c$. Jumps in N_{eff}^* served to reorder previously disordered regions when $S_i=1$, as indicated by

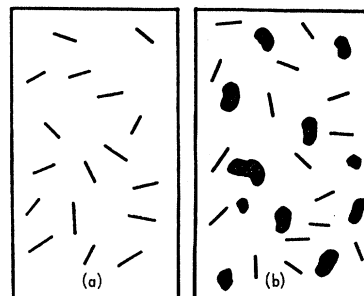


FIG. 15. Schematic representation of (a) minority strings in a $S_i=0$ configuration, (b) minority strings and ordered centers in a configuration with small $S_i (<0.2)$.

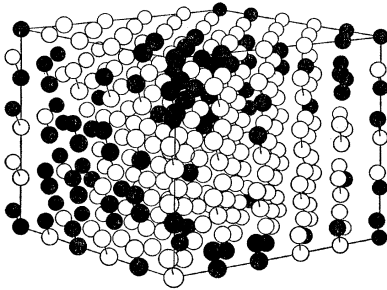


FIG. 16. An antiphase domain (APD) formed in the bcc system during ordering from $S_i=0$ at $\phi=1.8$ in a 10^4 -jump migration region. There are two types of APD's in the AB bcc system. Open symbols here denote site occupancy for one of these types (the largest domain); the filled symbols denote that for the other type (two fragments of adjacent domains). The larger domain is ~ 20 Å in diameter. About 450 atoms are contained in the region depicted.

$E_c^*/N_{\text{eff}}^* < 0$, while ordinary jumps served to disorder the lattice.

The order preserving, six-jump cycle suggested by Huntington and treated by Elcock and McCombie³⁵ was observed in ordered states. Data processing difficulties³¹ precluded an occurrence frequency analysis for this mechanism.

6. ANTIPHASE DOMAINS

Antiphase domains were located by stacking computer printed maps for successive (002) planes on a light table. Ball and spoke models of individual APD were then constructed. A model of an entire migration region was not built because as many as 2×10^6 lattice sites were involved. Figure 16 shows an APD established in the bcc system for $S_i=0$ and $\phi=2\phi_c$. Similar APD were evolved in the sc system. In the instances investigated, the migration region in an ALT lattice tended to be a mosaic of contiguous APD as was the case in two dimensions. Only isolated ordered nuclei were found in the NALT system. These different SRO structures directly correlate with the differences in the path structure illustrated in Fig. 14. An ordered nucleus in an $S_i=0$ environment was usually initiated by minority string eradication. Subsequent encounters with other minority strings produced additional nuclei in the immediate neighborhood of the primary nucleus. Contiguous APD would then usually form from this set of nuclei provided $\phi > \phi_c$.

The minority string nucleation mode was not unique. A vacancy starting its history in a homogeneously occupied subvolume produced a nucleus in a relatively inefficient "trial and error" fashion while executing a semirandom walk. When $S_i > 0$, ordered nuclei, appearing in the initial occupancy pattern, served as the principal nucleation centers for APD.

The occupancy map for a (002) plane through the migration region was similar to that shown in Fig. 17 for a two-dimensional system. Note that the APD cross

sections are strikingly similar to those observed by Marcinkowski and Brown³⁶ in an imperfect $B2$ superlattice (Fe_3Al) possessing isotropic APD boundaries.

Two experimental groups working independently and using different techniques conclude that ordering proceeds in Cu_3Au , a NALT system, by the continual formation of disjoint ordered nuclei up to the time of overlap. Weisberg and Quimby¹⁸ came to this conclusion on the basis of Young's modulus data. Nagy *et al.*¹⁴⁻¹⁶ decided this was the case from data on electrical resistivity, Hall coefficient, and thermoelectric power. This same picture is given by our calculations for NALT systems, but not for ALT systems. In ALT systems we find a strong tendency for the formation of contiguous APD rather than disjoint ordered nuclei.

7. VARIABLE ORDERING ENERGY

In two sets of calculations for the bcc system, the magnitude of the ordering energy for an atom was taken to be a linearly increasing function of the number of AB bonds n , associated with its position. The relation

$$\phi(n) = \phi^* - (n^* - n)x = v(n)/kT \quad (8)$$

was assumed, where $n^* = (z-1)$ is the largest number of AB bonds an atom adjacent to a vacancy can experience and x is the incremental change in ϕ per bond. The migration histories which resulted were the same as those associated with a constant ordering parameter, $\phi_{\text{eff}} = \phi^* + x$. Guttman⁴ shows that an upper bound on the variation of the ordering energy with the state of order is less than 2% for Cu_3Au . Within this range, the effects on Σ and β caused by varying the ordering energy were negligible except for one case. In disordering from $S=1.0$ at a temperature $T < T_c/2$, a 2% change in v caused a 10% reduction in Σ and β in the course of 3×10^4 jumps. A 10% change in v produced less than a 2% increase in the ordering rate (per jump) from $S_i=0$ at temperatures $T > T_c/2$.

8. SUMMARY AND CONCLUSIONS

The principle features of the order-disorder process in ALT and NALT systems, as given by the present study, are summarized in Table III. As was pointed out before,¹⁹ the rate of ordering is that per vacancy jump. Differences between ALT and NALT system behaviors spring from the circumstance that a long sequence of zero-energy change vacancy jumps can occur in a perfectly ordered NALT system but not in a perfectly ordered ALT system.

A number of results given by the Flinn-McManus model in this study are qualitatively consistent with experiment and other theoretical work. It is perhaps worthwhile to collect them in one place.

(1) The well-known effect of a decrease in the atomic diffusion coefficient for the ordered state relative to that extrapolated from the disordered state, reported for β

³⁵ E. W. Elcock and C. W. McCombie, *Phys. Rev.* **109**, 605 (1958); E. W. Elcock, *Proc. Phys. Soc. (London)* **73**, 250 (1959).

³⁶ M. J. Marcinkowski and N. Brown, *J. Appl. Phys.* **33**, 537 (1962).

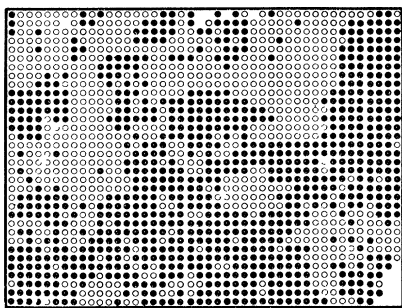


FIG. 17. Antiphase-domain outlines in a (002) cross section of the bcc-system migration region were similar to those shown here for a two-dimensional calculation. This pattern has the same general appearance of the antiphase-domain boundaries observed by Marcinkowski and Brown in the Fe_3Al imperfect $B2$ superlattice.

brass by Kuper *et al.*, is clearly given by the Flinn-McManus model. Specifically we observed a decrease in the vacancy diffusion coefficient. Upon assumption of the vacancy diffusion mechanism, this in turn implies a decrease in the atomic diffusion coefficients. In addition, we found that this effect begins above the critical temperature, as did Kuper *et al.*, and is not purely a LRO effect. However, at a given temperature $T < T_c$, the amount of diminution in D_v , due solely to the existence of an ordering energy in these calculations, was not as great as that Kuper *et al.* found for atomic diffusion.

(2) Recent experiments¹³⁻¹⁶ indicate that the initial ordering state in Cu_3Au (NALT system) consists of the continual formation of disjoint ordered nuclei. In subsequent stages these nuclei grow and coalesce. The Flinn-McManus model gives the same indication for NALT systems but not for ALT systems. In the latter case it predicts a strong tendency for contiguous APD formation in the migration region of a single vacancy followed by coalescence of these internally structured regions. In this regard an experiment in which β brass is (a) doped to give vacancy lifetimes of $\sim 10^4$ jumps, (b) quenched from above T_c , and (c) subsequently examined using transmission electron microscopy for domain structure would be informative.

(3) Brown and Cupshalk³⁴ directly observed vacan-

cies to be largely concentrated at APDB's in β brass. Nagy *et al.*¹⁴⁻¹⁶ suggest that a similar effect occurs in Cu_3Au during domain coalescence. In the latter case, the concentration of vacancies at APDB's was inferred from the existence of a lower activation energy for APD growth than for APD formation. This behavior, i.e., vacancy trapping at APDB was observed in this study and that of Ref. 1. In addition, we noted the removal of APD's, during coalescence, via vacancy movement along APD boundaries.

(4) The linear increase in the migration region volume with N , the number of vacancy jumps, is consistent with the initially linear time dependence of ordered nucleus volume growth predicted by Gross and Quimby.³⁷

(5) Marcinkowski and Brown³⁶ observed an irregular APD shape in an alloy (Fe_3Al) with isotropic APB and an imperfect $B2$ superlattice. This feature is also given by the present calculations wherein the APB's are isotropic and the appropriate superlattice is the $B2$ superlattice.

(6) Huntington suggested a six-jump cycle for vacancy diffusion which preserves LRO. A theoretical analysis of this mechanism by Elcock and McCombie³⁵ shows it should be important when $S \approx 1$. As mentioned in Sec. 5, this jump cycle was observed in the present study in the $S_i = 1$ experiments.

As stated in Sec. 2, the application of the Flinn-McManus model to a kinetic process is not strictly valid. It assumes that the jump probability is determined by the state of the crystal before and after the jump. This probability is actually determined by the initial state, and the activated state for the positional interchange between an atom and the vacancy. One should not, therefore, expect to obtain an accurate quantitative description of order-disorder kinetic processes using the Flinn-McManus model. However, the model does appear to give qualitatively significant results in that its description of the initial stage of order-disorder transitions is consistent with experimental observations on several physical characteristics, both microscopic and macroscopic in nature, as described above.

An absolute time scale cannot be defined in the Flinn-McManus model. Initially we were unable to estimate how the number of computer jumps might be related to the number of actual jumps. However, a way has been suggested to us of how to estimate the relative magnitude of the jump frequency, Γ_{FM} , associated with a Flinn-McManus calculation, and the jump frequency, Γ_{EX} , implicitly described by experimental data. This is found by noting that $1/\kappa\langle r^2 \rangle$, the reciprocal of the contraction factor for $\langle r^2 \rangle$, should be approximately proportional to Γ_{FM} . Similarly, the reciprocal of a diffusion coefficient contraction factor, $\kappa(D)$, obtainable from the data of Kuper *et al.* for β brass, should be approximately proportional to Γ_{EX} . The two propor-

TABLE III. Summary of characteristics observed in alternating and nonalternating systems for migration histories of $N \leq 3 \times 10^4$ jumps.

Characteristic	Alternating system	Nonalternating system
1. Over-all nature of order-disorder process	Local	Not local
2. Ordered center formation	Contiguous anti-phase domain	Disjoint ordered centers
3. Order-disorder rate	Fast	Slow
4. Migration extent relative to random walk	Smaller	\sim Same
5. Migration extent expansion	Linear in N	Linear in N
6. Energy change	Linear in N	Linear in N

³⁷ W. Gross and S. L. Quimby, see Ref. 11 of Ref. 13.

tionality factors involved should have nearly the same magnitude. Taking into account the existence of a vacancy concentration factor in $\kappa(D)$, not present in $\kappa(r^2)$, we found the ratio

$$\Gamma_{\text{FM}}/\Gamma_{\text{EX}} \simeq \kappa(D)/\kappa(r^2) = 3.6 \quad (9)$$

was constant on the interval $0.8 \leq \phi/\phi_c \leq 2$. This calculation was based on Girifalco's theoretical expressions for tracer diffusion coefficients and the vacancy concentration in ordered and disordered β brass. The result shown in Eq. (9) was determined using his numerical results for the diffusion of Cu. As was stated before, Girifalco's theory is in excellent agreement with the data of Kuper *et al.* This rough approximation suggests that no gross difference between the two jump frequencies exists, and that the Flinn-McManus method gives the correct ratio of jump frequencies for two different temperatures.

As shown here, the type of results one can obtain from a computer simulation experiment are clearly of interest in the study of transient states. However, these results cannot be fully utilized without knowing the associated absolute time scale. A sampling method in which an absolute time scale could be defined would be very

useful in general kinetics studies of systems involving the migration of two or more interacting species in a crystal. In an *operational* sense, however, this method should be no more complicated than the Flinn-McManus sampling method, in order to be a practicable method with respect to present day computers. An enormous number of sampling events must be performed in a full-scale simulation. The present study, for example, constitutes a meager beginning in kinetic process simulation of order-disorder transitions. One really needs to follow at least 10^6 jumps per vacancy in order to describe a sufficiently large part of the vacancy lifetime for the results to be immediately useful in the design and interpretation of experiments.

ACKNOWLEDGMENTS

The Monte Carlo computing and data-reduction programs were written by J. A. Delaney and Nancy R. Baumgardt. Data reduction was done by M. J. Schumacher and C. M. Schnur. The author wishes to thank Professor L. A. Girifalco and Dr. P. S. Rudman for interesting discussions and good advice. Special acknowledgment is due to Dr. Rudman for critically reading the first draft.

Electron and Phonon Scattering in GaAs at High Temperatures

A. AMITH, I. KUDMAN, AND E. F. STEIGMEIER*

RCA Laboratories, Princeton, New Jersey

(Received 3 December 1964)

The electrical resistivity ρ , the Seebeck coefficient Q , and the thermal conductivity κ , were measured in a series of GaAs samples in the temperature range 300–900°K. Values of Q were combined with room-temperature values of the Hall coefficient in order to derive the relative weights of the polar scattering ($\tau \sim E^r$, $0 \leq r \leq 0.5$) and the ionized-impurity scattering ($\tau \sim E^{3/2}$) in a self-consistent manner. The partial mobilities μ_P (polar mobility) and μ_I (ionized-impurity mobility) were then derived from the measured ρ . The Brooks-Herring formula for μ_I was found to overestimate screening effects. The temperature dependencies of these mobilities were $\mu_P \sim T^{-2.3}$ and $\mu_I \sim T^{3/2}$. Knowledge of the Fermi levels and of the degree of "mixing" of the two scattering mechanisms made it possible to assess exactly the electronic contributions to κ . It was found that κ_{lattice} was proportional to $T^{-1.25}$, and that it decreased as the free-carrier concentrations in the samples increased, thus showing the influence of scattering of phonons by electrons. The value of κ_{lattice} at the Debye temperature in the undoped material is used to confirm the contribution due to scattering of acoustical by optical phonons.

I. INTRODUCTION

THE electric¹⁻³ and thermoelectric⁴⁻⁶ properties of GaAs at elevated temperatures have been measured by many investigators. Measurements of thermal

conductivity, on the other hand, have been reported for room temperature⁷⁻¹¹ and below¹⁰⁻¹²; and there is only a single reference to their extension to elevated

* Present address: Laboratories RCA Ltd., Zurich 5, Switzerland.

¹ See, e.g., O. Madelung, *Physics of III-V Compounds* (John Wiley & Sons, Inc., New York, 1964), and references therein.

² H. Ehrenreich, *J. Appl. Phys. Suppl.* **32**, 2155 (1961).

³ D. J. Oliver, *Phys. Rev.* **127**, 1045 (1962).

⁴ J. J. Edmond, R. F. Broom, and F. A. Cunnell, *Report of Meeting on Semiconductors, Rugby* (The Physical Society, London, 1957), p. 109.

⁵ D. N. Nasledov, *J. Appl. Phys. Suppl.* **32**, 2140 (1961).

⁶ R. O. Carlson, S. J. Silverman, and H. Ehrenreich, *J. Phys. Chem. Solids* **23**, 422 (1962).

⁷ H. Weiss, *Ann. Physik* **4**, 121 (1959).

⁸ M. S. Abrahams, R. Braunstein, and F. D. Rosi, *J. Phys. Chem. Solids* **10**, 204 (1959).

⁹ J. Blanc, R. H. Bube, and L. R. Weisberg, *Phys. Rev. Letters* **9**, 252 (1962).

¹⁰ M. G. Holland, *Phys. Rev.* **134**, A471 (1964).

¹¹ M. G. Holland, *Physics of Semiconductors, Proceedings of the Seventh International Conference* (Dunod Cie., Paris, 1964), p. 713.

¹² N. N. Sirota, *Inzh. Fiz. Zh. Akad. Nauk Belorussk* **1**, 117 (1958).